Journal of Sound and Vibration (1999) **220**(2), 297–312
Article No. jsvi.1998.1924, available online at http://www.idealibrary.com on IDEAL

EXPERIMENTAL INVESTIGATION OF THE DAMPING OF STRUCTURAL VIBRATIONS BY VORTICITY PRODUCTION

P. M. Maung and M. S. Howe

Boston University, *College of Engineering*, 110 *Cummington Street*, *Boston*, *MA* 02215, *U.S.A.*

AND

G. H. McKinley

Harvard University, *Division of Engineering and Applied Sciences*, 29 *Oxford Street*, *Cambridge*, *MA* 02138, *U.S.A.*

(*Received* 23 *December* 1997, *and in final form* 12 *August* 1998)

An experimental investigation has been made of the damping of a plate vibrating at zero angle of attack to a nominally steady, high Reynolds number mean flow. The plate is perforated with a distribution of small circular apertures in which vorticity is produced by the unsteady loading of the plate. The kinetic energy of the vorticity is swept downstream by the flow. Damping occurs by the transfer of energy from the plate to the vortex field provided the Strouhal number $\omega R/U$, based on the radian frequency ω of the vibration, the aperture radius R and the mean stream velocity U, lies between about 0·4 and 0·8. The peak attenuation is of the order of 5 dB relative to an identical unperforated plate. The results are interpreted in terms of recent calculations of the unsteady flow through an aperture in the presence of mean flow, and are expected to be relevant to the alleviation of fatigue failure of aerodynamic control surfaces such as jet nozzle flaps.

1. INTRODUCTION

Vorticity is produced by a vibrating solid surface. The rate of production is greatest where the pressure and velocity in the fluid change rapidly, such as at corners and sharp edges. For certain conditions the kinetic energy of the vortex flow is derived from the work done on the fluid by the moving surface, and there is an irreversible transfer of energy to the fluid. The mechanism is very similar to that involved in the conversion of *acoustic* energy into vortical kinetic energy when sound causes vorticity production at an edge: vorticity diffuses from the edge by viscous action and the sound is damped [1–3]. If the fluid is at rest relative to the surface the dissipation is caused by the non-linear convection of vorticity from the surface and subsequent thermoviscous damping, both of which are

0022–460X/99/070297 + 16 $30.00/0

weak because the growth of vorticity of one sign (and, therefore, of substantial levels of vortical kinetic energy) tends to be inhibited when the motion is periodic. In the acoustic case it is known [4–16] that the damping can be greatly increased by the presence of a high Reynolds number mean flow. Viscosity is now important only very close to an edge, where vorticity diffuses from the surface and is then swept away by the flow, its kinetic energy being permanently lost by the sound.

Practical devices for attenuating sound by this means usually involve *bias* or *grazing* flow perforated screens. In the bias flow case a mean pressure difference is maintained across the screen producing a steady flow through the apertures. Damping is caused by the modulation of vorticity production in the mean jet flows through the apertures by impinging sound [6, 7, 12, 14–16]. A grazing flow screen works in a similar way: unsteady motion produced by the sound in the apertures generates vorticity which is convected downstream by the tangential flow over the screen. High acoustic intensities are usually accompanied by significant structural vibrations, and since near field (non-acoustic) pressure fluctuations produced by a vibrating body can also modulate vorticity production, it is likely that the vibrations of a perforated structure are also damped by vorticity production. This possibility has been confirmed theoretically [17, 18] for bending waves on a bias flow elastic plate, or when a bending wave impinges on the edge of a plate in the presence of a tangential mean flow. These studies indicated that the damping can be comparable with that normally achieved by heavily coating the vibrating plate with an elastomeric damping material. The efficiency of damping by the bias flow screen can be optimized for any particular frequency by adjusting the bias flow speed in the perforates. This is not generally possible for perforated screens in a tangential flow environment. Either of these configurations, however, provides a possible mechanism for suppressing the large amplitude vibrations induced in practical flow control devices by large scale flow instabilities, such as those experienced by the jet engine external nozzle flaps of certain military aircraft [19–21].

In this paper we describe the results of an experimental investigation aimed at assessing the likely magnitudes of the structural damping that can be achieved by vorticity production. The case considered here is of damping by the *passive* production of vorticity in the apertures of a perforated plate which vibrates while immersed in a water channel in the presence of a tangential mean flow of speed $U \approx 1$ m/s. Vibration damping measurements were made using several cantilevered, thin steel plates homogeneously perforated with circular apertures of radius $R = 1/8$ in. and with respective fractional open areas $\alpha = 0{\cdot}0135, 0{\cdot}03, 0{\cdot}05$ and $0{\cdot}1$. In all of these cases maximum damping of up to 5 dB (relative to an identical unperforated plate with the same vibrational input power) was obtained at a *Strouhal number* $\omega R/U$ between about $0{\cdot}4$ and $0{\cdot}8$, where ω denotes the radian frequency of vibration. Intervals of *negative* damping were observed at higher Strouhal numbers; in such cases the forced vibrations of the plate are augmented by energy extracted from the mean flow. These conclusions are consistent with elementary analytical models of the hydrodynamics of the unsteady aperture motions in the presence of mean flow [22–24], in which the mean shear layer across

an aperture is modelled by a vortex sheet, but it is not clear to what extent these models are applicable in the present case.

These simple models are discussed in section 2. The experimental set-up and the test procedure are described in section 3, and damping measurements are reported in section 4. The experimental results are discussed for several fractional open areas, with greatest attention given to the case $\alpha = 0{\cdot}0135$, which is likely to be the most relevant in applications, where only small fractional open area ratios are likely to be acceptable.

2. THEORETICAL BACKGROUND

Consider a thin plate containing a circular aperture (of radius R) vibrating normal to its surface with small amplitude at radian frequency ω (with time dependence $\propto e^{-i\omega t}$) in the presence of a grazing mean flow in the x_1-direction (Figure 1). In the general case the mean velocities $U_\pm$ respectively above and below the plate will be different, and in the absence of oscillations there will be a mean shear layer across the plane of the aperture. The periodic motion of the plate produces uniform, mean pressures $p_\pm e^{-i\omega t}$ on the upper and lower faces of the plate, as a result of which fluid is forced through the aperture at a volume flux rate $Q e^{-i\omega t}$ (in the positive x_2-direction in the figure) given by

$$Q = \frac{K(\omega)[p_+ - p_-]}{i\rho_0\omega}, \tag{1}$$

where ρ_0 is the mean fluid density, and the frequency dependent coefficient K is the *Rayleigh conductivity* of the aperture. In the absence of mean flow in an ideal

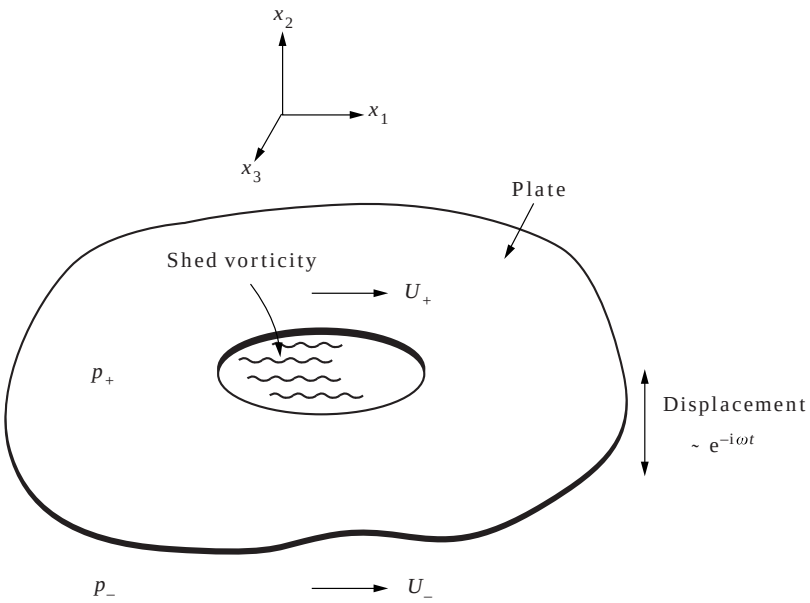

Figure 1. Tangential mean flow past a circular aperture in a vibrating plate.

fluid the value of K depends only on the *shape* of the aperture and the thickness of the plate. For a circular aperture in a plate of infinitesimal thickness $K = 2R$.

Because of the tangential motion, vorticity is shed from the edge of the aperture and carried downstream by the mean flow. This implies that there is an exchange of energy between the fluid and the vibrating plate, and that K is now a *complex* function of the frequency ω, which is usually expressed in the form

$$K(\omega) = 2R(\Gamma(\omega) - \mathrm{i}\Delta(\omega)), \tag{2}$$

where Γ and Δ are real. If Π denotes the rate of transfer of energy from the plate to the fluid, then [18]

$$\Pi = \frac{-\operatorname{Im}\{K(\omega)\}|p_+ - p_-|^2}{2\rho_0\omega} \equiv \frac{R\Delta(\omega)|p_+ - p_-|^2}{\rho_0\omega}, \tag{3}$$

which is positive provided $\Delta(\omega) > 0$ (for $\omega > 0$).

Figure 2 illustrates the dependencies of Γ and Δ on the *Strouhal number* $\omega R/U$ calculated by Scott [22] for an aperture in a plate of zero thickness in the two extreme cases of (1) one-sided flow, $U_+ = U$, $U_- = 0$, and (2) two-sided uniform flow, $U_+ = U_- \equiv U$. According to equation (3), in the intervals where $\Delta > 0$, vibrational energy is transferred to the fluid. For one sided flow this occurs at Strouhal numbers less than about 2; for two sided, uniform flow it occurs over a large number of discrete frequency intervals. In obtaining these results, Scott considered the extreme limit of infinite Reynolds number, when the mean shear layer across the apeture could be modeled by a *vortex sheet* which was linearly perturbed by motion of the plate.

In the experiments considered in this paper, the vibrating plate is immersed in water at zero mean angle of attack to a nominally uniform mean flow. Thus, it might be expected that case (b) of Figure 2 would provide an appropriate model for interpreting the exchange of energy between the plate and the flow. However, it turns out that this two sided-flow model is valid only for plates of very small thickness compared to the aperture radius R. Although numerical predictions of $K(\omega)$ for a circular aperture in a thick plate are not available, it is found [24] that, apart from a change of scale on the frequency axis, the results shown in Figure 2 are also applicable to a *rectangular* aperture. However, it is shown in reference [24] that for two-sided uniform flow over a rectangular aperture in a plate of moderate thickness, the frequency dependence of the conductivity is actually more like case (a) of Figure 2 (one-sided flow). This is illustrated in Figure 3 for a rectangular aperture of length $2s$ and breadth $4s$ (out of the plane of the paper) in a plate of thickness $h = 0{\cdot}2s$. The reason for this critical dependence on thickness is easily understood. For a plate of zero thickness in a uniform mean flow, there is no mean shear layer (vortex sheet) across the aperture in the limit of infinite Reynolds number, and the undisturbed motion is therefore *stable*. For finite thickness, however, a vortex sheet will span each face of the aperture, as indicated in the upper part of Figure 3, thereby making the aperture motion unstable. Numerical results discussed in reference [24] indicate that the unstable motion becomes similar to that for one-sided flow when the plate thickness exceeds about one tenth of the aperture diameter.

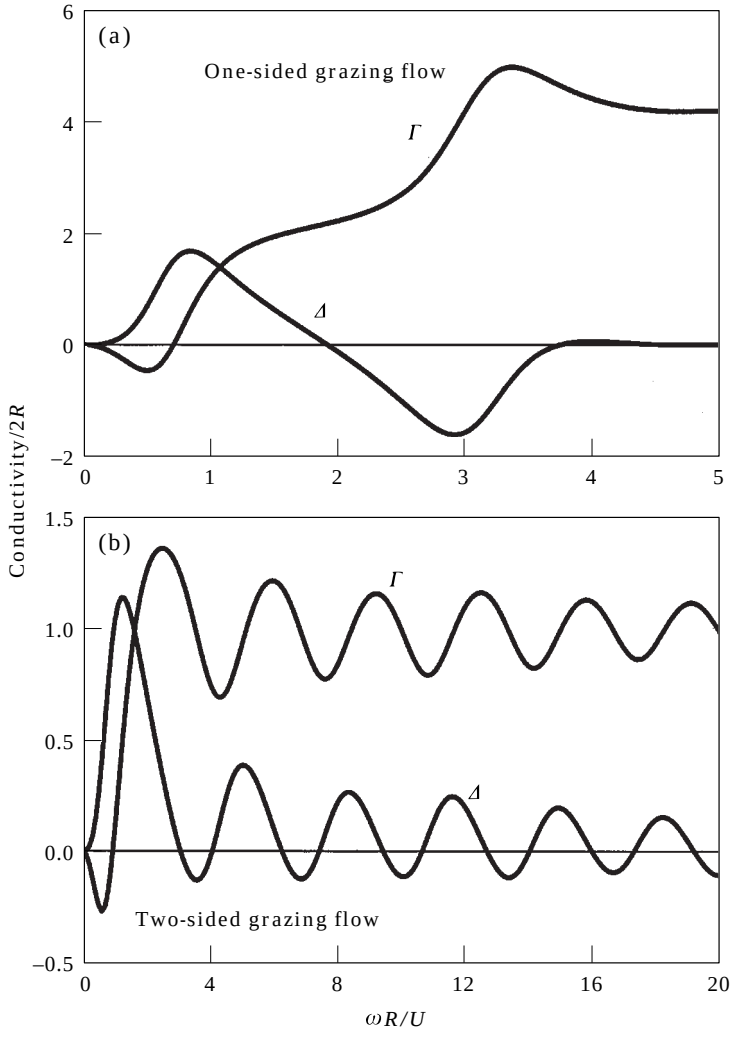

Figure 2. Conductivity of a circular aperture in grazing flow: (a) $U_+ = U$, $U_- = 0$; (b) $U_+ = U_- = U$.

3. DESCRIPTION OF THE EXPERIMENT

3.1. APPARATUS

The experiment was conducted in the 20 ft long low speed water channel at Harvard University. The channel is 1.5 ft wide and 3 ft high, and the water depth is about 6·75 in. at the maximum flow rate of approximately 100 gallons/min, corresponding to a mean stream speed $U = 0{\cdot}8 - 0{\cdot}85$ m/s. This velocity was measured directly by observation of particle traces on the surface of the water.

The experiments were performed using a set of interchangeable unperforated and perforated rectangular steel plates aligned at zero mean angle of attack to the flow. The plates are of thickness 1/32 in. and have span 11 in. (transverse to the flow direction) and chord 6 in. The perforated plates had fractional open areas $\alpha = 0{\cdot}0135, 0{\cdot}03, 0{\cdot}05, 0{\cdot}1$, and were formed by drilling a uniform distribution of

circular apertures of radius $R = 1/8$ in. Each test plate is cantilevered about its leading edge, along which it is bolted to a 1/8 in. thick, horizontal steel bar placed within the water flow at a depth that could be varied between 1·75–4·25 in., the bar being strong enough to prevent twisting during plate vibration.

A Ling Dynamic System V203 shaker was mounted on a rigid support above the plate and connected to the midspan of the plate near the trailing edge by a 1/4 in. diameter vertical aluminum connecting rod. A Tektronix CFG280 function generator was used to drive the shaker at prescribed values of the radian frequency ω. The connecting rod is rigidly attached to the plate, whose motion at the point of attachment could therefore be measured by means of a high sensitivity accelerometer (Kistler 863485) mounted on the rod above the water level. This was checked in the absence of water by operating the shaker at fixed input frequency and amplitude and comparing accelerometer readings when mounted on the connecting rod and when mounted directly on the plate. A PC-based data acquisition system was used to store simultaneous measurements of the accelerometer output $a(t)$, and the voltage $V(t)$ and current $I(t)$ delivered to the shaker. The arrangement is illustrated schematically in Figure 4, and described in greater detail in reference [21].

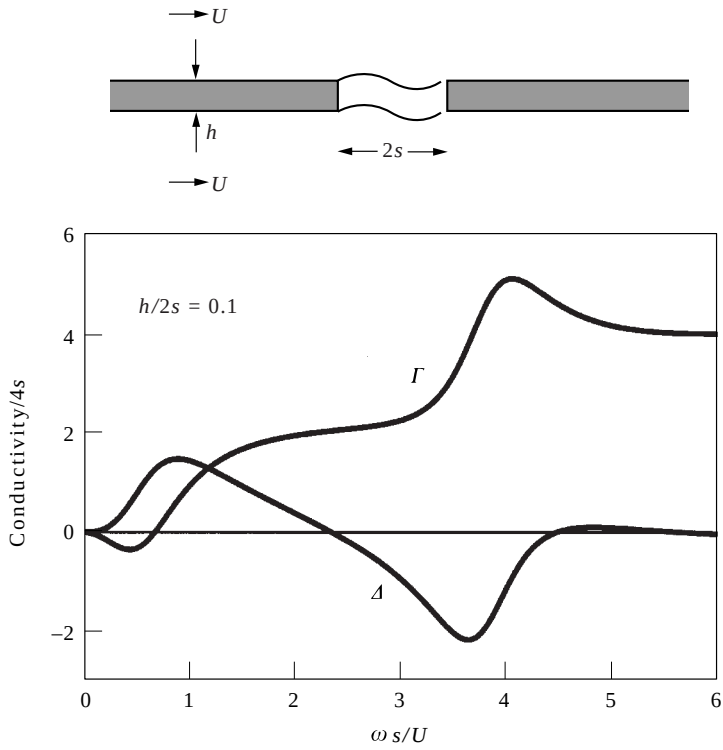

Figure 3. The conductivity of a rectangular aperture of streamwise length $2s$ and breadth $4s$ (out of the paper) in a plate of thickness $h = 0{\cdot}2s$ in the presence of two-sided uniform flow at speed U.

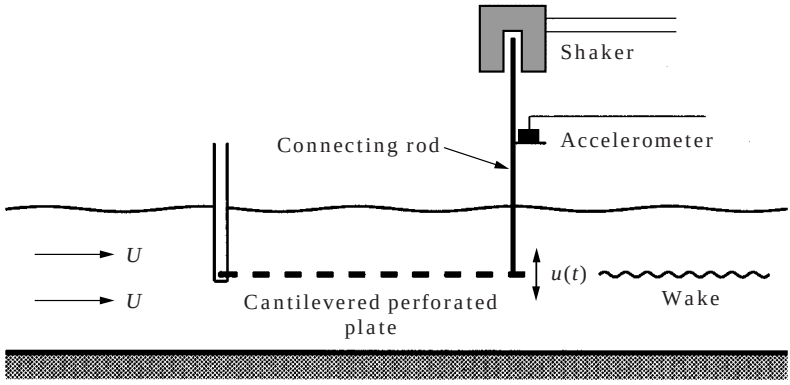

Figure 4. Schematic illustration of the test configuration.

3.2. PROCEDURE

The mean flow speed was maintained steady in the range $U = 0{\cdot}8$–$0{\cdot}85$ m/s, and the shaker was driven sinusoidally at selected frequencies $f = \omega/2\pi$ between 10 and 90 Hz. Over this range the Strouhal number $S = \omega R/U$ varies from 0·2 to 2·15, where, according to Figures 2 and 3, vorticity production is expected to provide a significant level of vibration damping.

Spectral analysis of the accelerometer readings indicates that the response of the plate is perfectly sinusoidal except at the lower end of the frequency range and a few other selected points. Even at these exceptional points, however, the signal is nearly sinusoidal with some added noise distortions (see Figures 5 and 6). The plate displacement $u(t)$ as a function of time can be calculated from the accelerometer readings by integration of the formula

$$\frac{\mathrm{d}^2u}{\mathrm{d}t^2} = a(t). \tag{4}$$

This was done numerically using a trapezoidal procedure and 1024 data points sampled over a three period duration. This time period was found to be large enough to provide a stable frequency spectrum, with adequate low frequency resolution.

The current and voltage delivered to the shaker were analyzed in a similar manner. When conditions vary sinusoidally, the power delivered to the shaker is the product of the voltage $V(t) = v_0 \cos(\omega t)$ and current $I(t) = \hat{I} \cos(\omega t + \phi)$, and the average power Π is given by

$$\Pi = v_0 \hat{I} \cos \phi. \tag{5}$$

The voltage was measured across the electrical leads coming out of the shaker. The current $I(t)$ was determined from Ohm's law and the measured voltage drop across a 1Ω resistor placed in series. Instead of assuming perfectly sinusoidal variations and using equation (5), the average power was calculated from the

actual sampled values of $V(t)$, $I(t)$ over a three period interval by means of the formula

$$\Pi = \frac{\Sigma_n V(t_n) I(t_n) \Delta t}{\Sigma_n \Delta t}, \tag{6}$$

where Δt is the interval between successive sampling times t_n. This method of computation minimizes the influence of random fluctuations present in the peak to peak measurements.

The plate and the connecting rod to the shaker may be regarded as a linear system executing forced oscillations at frequency ω. The total power dissipated per unit input power to the shaker is proportional to the ratio u_p^2/Π_p, where the subscript p refers to values for the perforated plate, and u_p^2 is the mean square

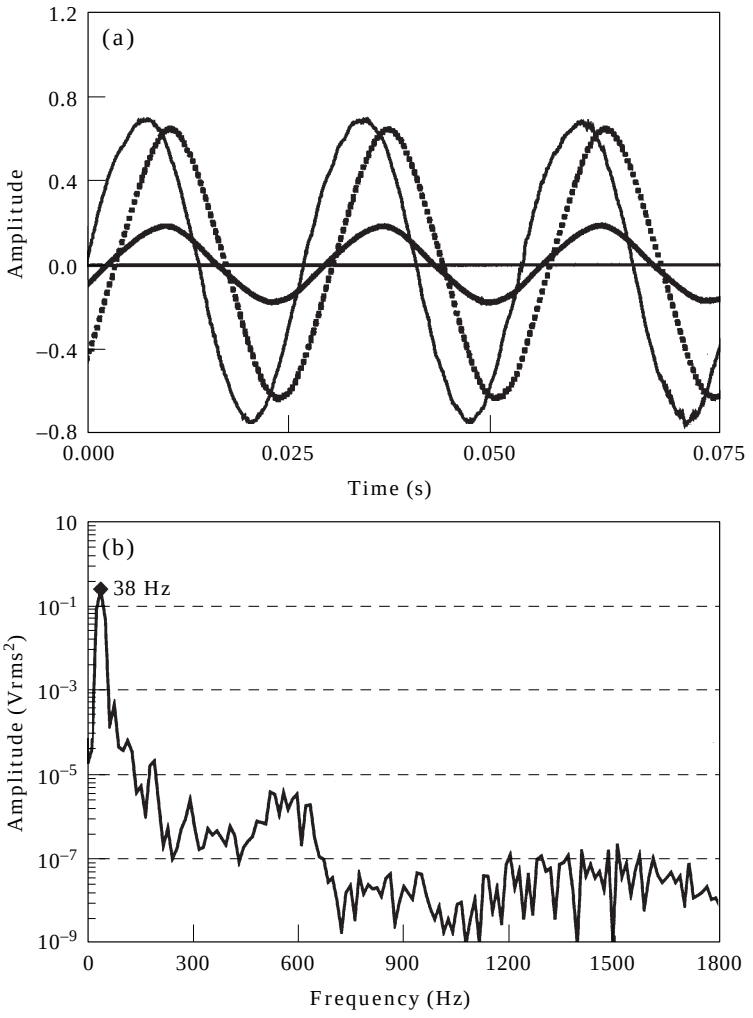

Figure 5. The 1·35% plate: (a) shaker current (—) (A) and input voltage (· · ·), and accelerometer voltage (——) for $f = 38$ Hz and $v_o = 124$ mV; (b) frequency spectrum of the accelerometer reading at a shaker frequency of 38 Hz.

displacement of the plate. The damping of the coupled plate-shaker system afforded by vorticity production in the perforates is therefore determined by

$$10 \times \log_{10}\left(\frac{u_o^2}{u_p^2}\frac{\Pi_p}{\Pi_o}\right), \text{dB}, \tag{7}$$

where the subscript o refers to the *unperforated* plate.

4. EXPERIMENTAL RESULTS

To assess the importance of vibration amplitude on damping, measurements were made at two different voltage input amplitudes, v_o, to the shaker of 124 and 174 mV (corresponding, practically, to a doubling of the input power at the higher voltage), which could be held stable throughout the whole range of test frequencies. It will be seen from the results that the input amplitude has only a minor influence on the measured damping. The input frequency was varied over over the range $10 < \omega/2\pi < 90$ Hz in increments of 2–5 Hz. Smaller increments were used where significant damping was observed. For each frequency the measured displacement of the plate at the trailing edge (u) and the average input power Π were measured during four different experimental runs to ensure repeatability and consistency of the measurements. The mean values of these results were then used to compute the damping. For a given fractional open area, the shaker input voltage amplitude v_o was constant to within $\pm 3\%$, while the current varied with the driving frequency f. The accuracy of the power measurements was confirmed by direct comparison with performance characteristics supplied by the shaker manufacturer. As an additional precaution to ensure the validity and consistency of the measurements, a second test was conducted after an interval of a few days, and additional checks (described below) were performed for the plate with the smallest fractional open area of 1·35%.

4.1. THE 1·35% PERFORATED PLATE

The most extensive tests were conducted on the 1·35% perforated plate. Four separate tests were performed, each involving the measurement of the displacement and average input power on eight separate occasions with the same flow velocity U, frequency f and input voltage amplitude v_o. The flow velocity and frequency variables were reset before each test, and all of the measurements were performed within a 2 week time frame. The measured power and displacement signals were stable over the entire frequency range, and spectral analysis revealed that the shaker current and voltage remained sinusoidal at all measurement points. The stability of the signal is demonstrated in Figure 5(a) and Figure 6(a), which show digitized sample readings of $I(t)$ and $V(t)$ for two different frequencies. The accelerometer readings contain a broader spectrum of frequencies, however. The distortion (non-sinusoidal response) of the plate motion was negligible except at very low frequencies. Figure 5(a) shows conditions at $f = 38$ Hz, where the input voltage, current and the acceleration are all sinusoidal; the acceleration frequency spectrum shown in Figure 5(b) is dominated by this frequency. This is the case

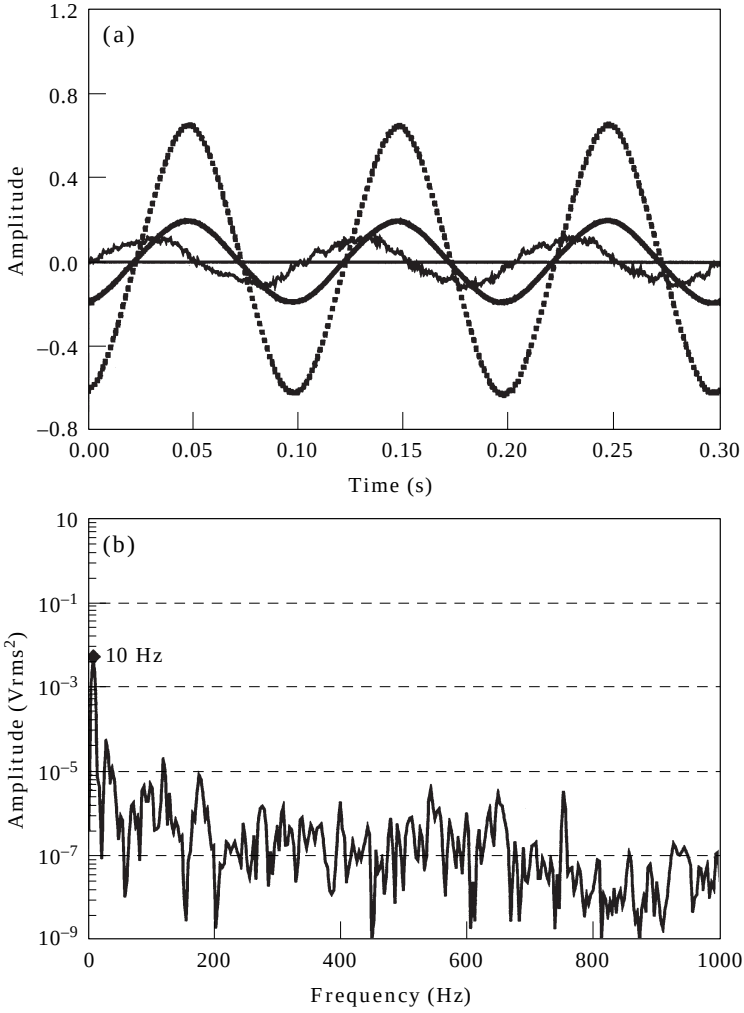

Figure 6. The 1·35% plate: (a) shaker current (—) (A) and input voltage (· · ·), and accelerometer voltage (——) for $f = 10$ Hz and $v_o = 124$ mV; (b) frequency spectrum of the accelerometer reading at a shaker frequency of 10 Hz.

for the majority of the measured frequencies. However, at low frequencies, such as that illustrated in Figure 6 for $f = 10$ Hz, the essentially sinusoidal response of the plate is contaminated by high frequency noise. The acceleration spectrum [Figure 6(b)] is still diminated by the peak at 10 Hz, however, which is about 20 dB above the noise. A comparison of the accelerometer measurements for the perforated and unperforated plates reveals that the noise level in the displacement readings is mainly a function of frequency and is not significantly dependent on the fractional open area.

The damping [calculated from the definition (7)] for $\alpha = 0{\cdot}0135$ is plotted in Figure 7 as a function of the aperture Strouhal number $\omega R/U$ for the two different peak input voltages $v_o = 124$ and $v_o = 174$ mV. The two results differ in detail, but are similar in overall appearance, confirming that in a first approximation the

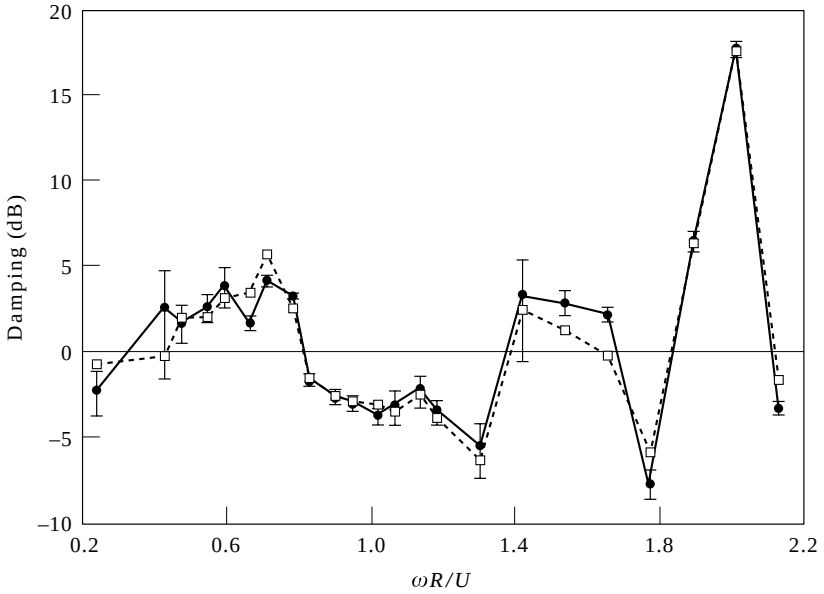

Figure 7. Measured damping (dB) of the 1·35% perforated plate for $v_o = 124$ (●) and 174 mV (□).

vibrating system may be treated as a linear oscillator. An error analysis, taking account of both precision and bias errors [25], was conducted on the damping comparison variables and the estimated uncertainties in the measured results are indicated by the error bars in Figure 7. Thus, for all practical purposes the results for the two input voltages may be regarded as essentially identical, as expected for a linear system.

Since the ratio plate thickness/aperture diameter $\equiv h/2R = 0{\cdot}125 > 0{\cdot}1$, it might be expected that the frequency dependence of the attenuation would be similar to that shown in Figure 3. However, the results of Figure 7 are more like those shown in Figure 2(b) for two-sided flow past an aperture in a plate of infinitesimal thickness. But the similarity is only qualitative, the observed frequency intervals of positive damping being much smaller. In the Strouhal number range $0{\cdot}4 < S < 0{\cdot}8$ the attenuation is typically about 3 dB, and attains a maximum of 5·7 dB at $S \approx 0{\cdot}7$.

The anomalously large damping which occurs in Figure 7 near $S = 2$ is believed to be associated with a resonance of the structural support at $f \approx 85$ Hz, since it occurs where the plate displacement is very small. To check this the test was repeated after first sealing the apertures with tape. If the tape can be regarded as effectively rigid there should be no damping due to the presence of the apertures, but any anomalies at a structural resonance are still likely to be present. Figure 8 compares the measured attenuations for the perforated and taped plates. Taping the apetures is seen to effectively eliminate the measured damping over most of the frequency range, except at the high frequencies. The small, but finite damping at lower frequencies for the taped plate can be attributed to the interaction of flexural motions of the tape over the apertures with the flow. It may therefore be

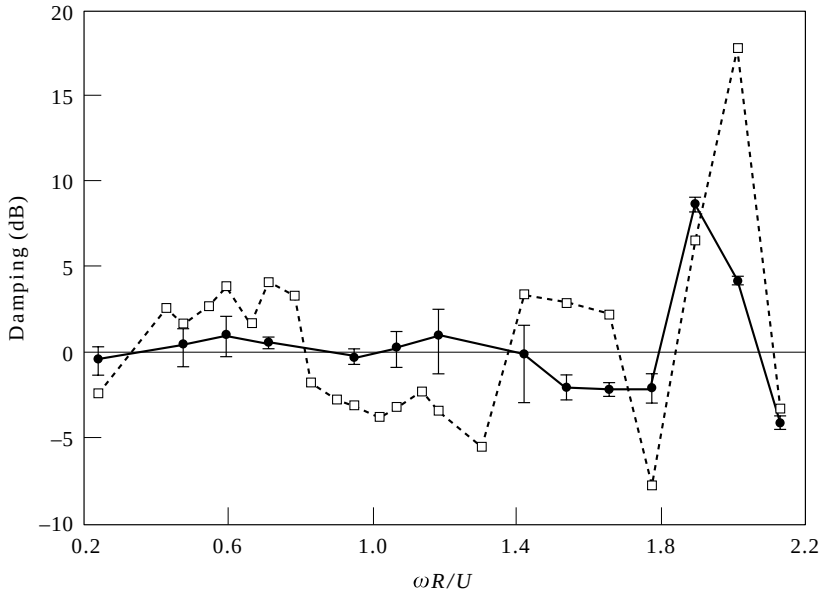

Figure 8. Comparison of the measured damping (dB) of the taped 1·35% perforated plate (solid curve) and the untaped plate (dashed) for $v_o = 124$ mV.

concluded that, except for high frequencies, say $f > 50$ Hz, vorticity production in the perforates is the major source of damping when comparing the measured responses of the perforated and unperforated plate.

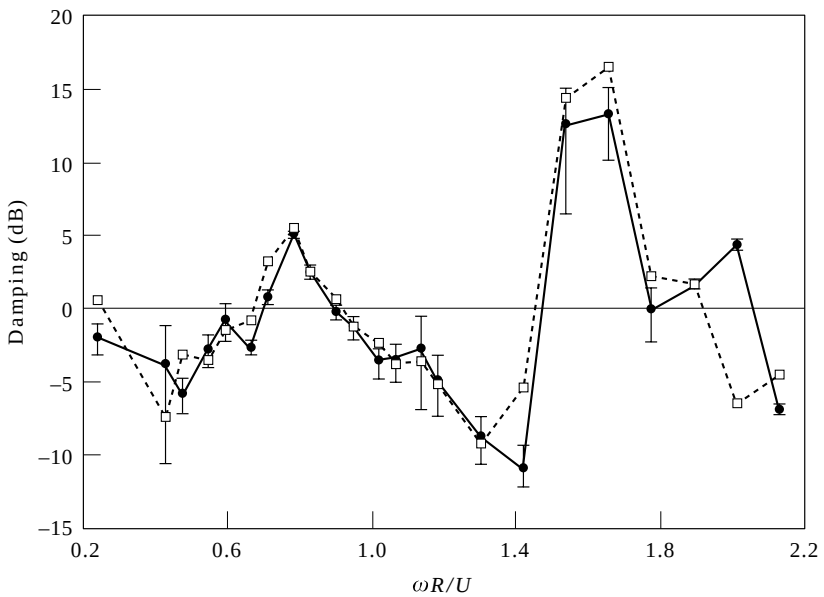

Figure 9. Measured damping (dB) of the 3% perforated plate for $v_o = 124$ (●) and 174 mV (□).

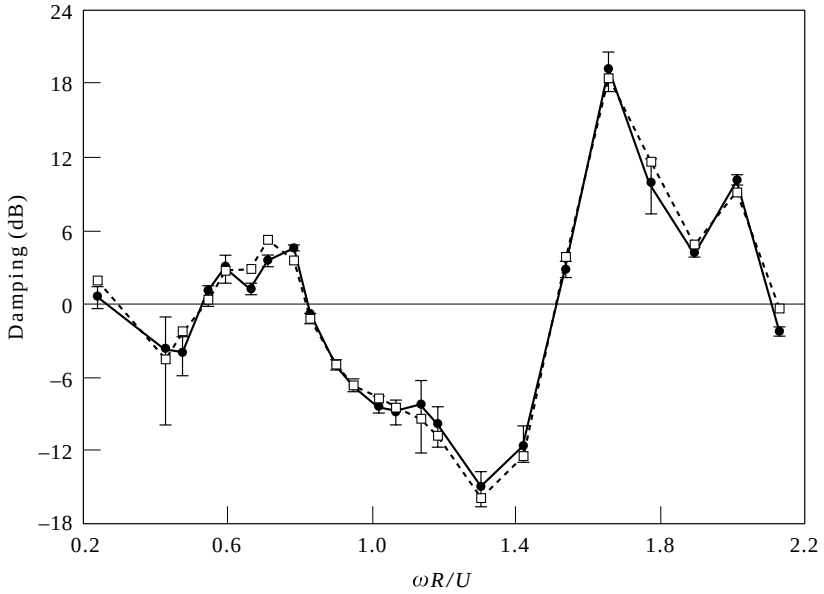

Figure 10. Measured damping (dB) of the 5% perforated plate for $v_o = 124$ (●) and 174 mV (□).

4.2. DEPENDENCE OF DAMPING ON FRACTIONAL OPEN AREA

Figures 9–11 illustrate the damping measured for plates with fractional open areas $\alpha = 0{\cdot}03$, $0{\cdot}05$ and $0{\cdot}10$ respectively. The results are quantitatively similar to those discussed above for $\alpha = 0{\cdot}0135$, however the low Strouhal number interval of significant damping progressively decreases in width as α increases, and the system exhibits "negative damping" over most of the low frequency domain, i.e., the oscillations are amplified by vorticity production.

The average damping for the 3% perforated plate is about 3 dB and occurs over the range $0{\cdot}7 < S < 0{\cdot}9$, which is much narrower than for the 1·35% plate. In this interval a peak attenuation of about 5·5 dB occurs at $S \approx 0{\cdot}8$, corresponding to $f = 33$ Hz. The very large measured damping in the region $S > 1{\cdot}5$ must again be attributed to a structural resonance. Similar comments apply to the 5% perforated plate. The low frequency region of damping occurs in the range $0{\cdot}5 < S < 0{\cdot}8$, with a maximum of 5·2 dB at $S \approx 0{\cdot}7$.

For the plate with the highest open area ratio of 10%, Figure 11 shows that the low Strouhal number interval of positive damping is now confined to the very small range $0{\cdot}7 < S < 0{\cdot}8$, and the maximum damping is 4 dB. For most frequencies the plate is negatively damped. This suggests that the large fractional open area the plate has a significant influence on the mechanical stiffness of the plate, causing it to exhibit a complex mode of deflection that is basically destabilized by the presence of the apertures. When the fractional open area is as large as 10% the plate no longer behaves as a simple forced oscillator with one degree of freedom. A progressive increase in open area causes a gradual reduction in plate stiffness, which ultimately allows the plate to vibrate in a more complex manner than the envisaged simple cantilever mode discussed above, thereby

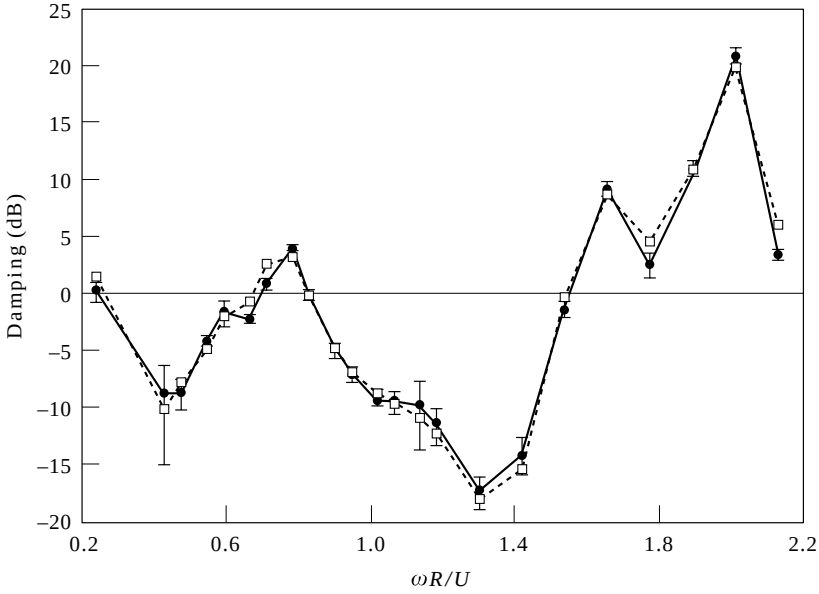

Figure 11. Measured damping (dB) of the 10% perforated plate for $v_o = 124$ (●) and 174 mV (□).

introducing phase differences between the fluid structure interactions at different apertures.

5. CONCLUSION

In this paper we have described an experiment in which the production of vorticity within the apertures of a vibrating plate immersed in a mean flow has resulted in a net exchange of energy between the flow and the vibrating plate. When vibration damping occurs the kinetic energy of the vorticity is supplied by the plate and swept away by the mean flow. The present experiment relies on the *passive* production of vorticity, and accordingly exhibits ranges of Strouhal numbers (based on mean flow velocity and aperture radius) where the damping can be negative.

Our results for vibrating steel plates in a water channel show that passive vorticity production in the perforates of a vibrating perforated plate can cause significant vibration damping (5 dB or more) for Strouhal numbers in the range 0·4 to 0·8. The width of this Strouhal number range decreases with increasing fractional open area; for the perforated plates studied here the broadest band of attenuation frequencies was obtained for a fractional open area of 1·35%. The solid curve in Figure 12 represents a "best fit" approximation to all of the data in this low Strouhal number range for this plate configuration.

The results give encouraging support to the possibility of controlling or suppressing unwanted vibrations of a structure in a mean flow by introducing a modest degree of surface perforations where vorticity production can occur. The passive vorticity generation configuration examined in this paper provides little or

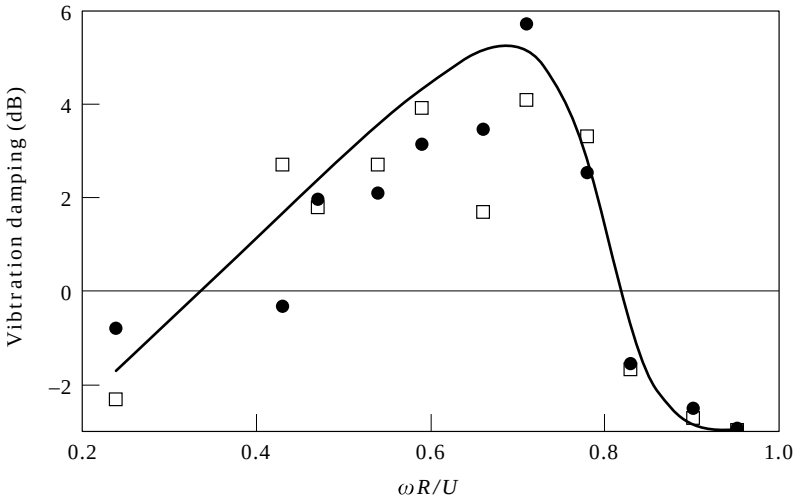

Figure 12. "Best fit" representation of the damping of the 1·35% perforated plate (□, $v_o = 124$; ●, 174 mV).

no control of the frequency at which the damping is maximal. However, the same mechanism is responsible for damping by vorticity production in the apertures through which a mean flow is maintained by "blowing" or "suction". For such an arrangement the "bias flow" velocity within an aperture can be adjusted to optimize damping at any desired frequency. Non-passive devices of this kind are known to be very effective in the damping of sound.

ACKNOWLEDGMENTS

This work is sponsored by the Air Force Office of Scientific Research under Grant No. F49620-96-1-0098, administered by Major Brian Sanders. The authors acknowledge with thanks the help and advice of Dr Mel King of Boston University. The support of Professor Albert Gold in granting permission to use facilities of the Division of Applied Sciences at Harvard is gratefully acknowledged.

REFERENCES

1. B. T. Zinn 1970 *Journal of Sound and Vibration* **13**, 347–356. A theoretical study of nonlinear damping by Helmholtz resonators.
2. T. H. Melling 1973 *Journal of Sound and Vibration* **29**, 1–65. The acoustic impedance of perforates at medium and high sound pressure levels.
3. A. Cummings 1983 *American Institute of Aeronautics and Astronautics Paper* 83-0739. Acoustic nonlinearities and power losses at orifices.
4. P. D. Dean and B. J. Tester 1975 *National Aeronautics and Space Administration Contractor Report* CR-134998. Duct wall impedance control as an advanced concept for acoustic suppression.
5. D. Bechert, U. Michel and E. Pfizenmaier 1977 *American Institute of Aeronautics and Astronautics Paper* 77-1278. Experiments on the transmission of sound through jets.

6. D. W. Bechert 1979 *American Institute of Aeronautics and Astronautics Paper* 79-0575. Sound absorption caused by vorticity shedding, demonstrated with a jet flow.
7. M. S. Howe 1980 *Journal of Sound and Vibration* **70**, 407–411. The dissipation of sound at an edge.
8. M. S. Howe 1979 *Proceedings of the Royal Society of London* **A366**, 205–233. On the theory of unsteady high Reynolds number flow through a circular aperture.
9. M. S. Howe 1980 *Proceedings of the Royal Society of London* **A370**, 523–544. On the diffraction of sound by a screen with circular apertures in the presence of a low Mach number grazing flow.
10. I. L. Vér 1982 *Paper presented at* 1982 *meeting of the Federation of the Acoustical Societies of Europe*; *Göttingen*. Perforated baffles prevent flow-induced acoustic resonances in heat exchangers.
11. A. M. Cargill 1982 *Journal of Fluid Mechanics* **121**, 59–105. Low frequency sound radiation and generation due to the interaction of unsteady flow with a jet pipe.
12. M. S. Howe 1984 *Institute of Mathematics and its Applications*, *Journal of Applied Mathematics* **32**, 187–209. On the absorption of sound by turbulence and other hydrodynamic flows.
13. I. L. Vér 1990 *Noise Control Engineering Journal* **35** (Nov/Dec), 115–125. Practical examples of noise and vibration control: case history of consulting projects.
14. I. J. Hughes and A. P. Dowling 1990 *Journal of Fluid Mechanics* **218**, 299–336. The absorption of sound by perforated linings.
15. Y. Fukumoto and M. Takayama 1991 *Physics of Fluids* **A3**, 3080–3082. Vorticity production at the edge of a slit by sound waves in the presence of a low Mach number bias flow.
16. A. P. Dowling and I. J. Hughes 1992 *Journal of Sound and Vibration* **156**, 387–405. Sound absorption by a screen with a regular array of slits.
17. M. S. Howe 1992 *Journal d'Acoustique* **5**, 603–620. On the damping of structural vibrations by vortex shedding.
18. M. S. Howe 1995 *European Journal of Applied Mathematics* **6**, 307–328. The damping of flexural and acoustic waves by a bias-flow perforated elastic plate.
19. J. M. Seiner, M. K. Ponton, O. C. Pendergraft Jr, J. C. Manning and M. L. Mason 1990 *American Institute of Aeronautics and Astronautics Paper* 90-1910. External nozzle flap dynamic load measurements on F-15 S/MTD mode.
20. J. M. Seiner, J. C. Manning, F. J. Capone and O. C. Pendergraft Jr 1992 *American Society of Mechanical Engineers Journal of Engineering for Gas Turbines and Power* **114**, 816–829. Study of external dynamic flap loads on a 6 percent B-1B model.
21. P. Maung and M. S. Howe 1997 *American Institute of Aeronautics and Astronautics Paper* 97-0576. Vibration damping of jet nozzle flaps by vorticity production.
22. M. I. Scott 1994 M.Sc. Thesis, Boston University. The Rayleigh conductivity of a circular aperture in the presence of grazing flow.
23. M. S. Howe, M. I. Scott and S. R. Sipcic 1996 *Proceedings of the Royal Society of London* **A452**, 2303–2317. The influence of tangential mean flow on the Rayleigh conductivity of an aperture.
24. M. S. Howe 1997 *Journal of Fluids and Structures* **11**, 351–366. Influence of wall thickness on Rayleigh conductivity and flow-induced aperture tones.
25. T. G. Bechwith, R. D. Maragoni and J. H. Lienhard 1993 *Mechanical Measurements*, 5th edn. Reading, MA: Addison–Wesley.